

Variable Frequency Pulse Control of Llc Resonant Dc-Dc Converter Using Rbfnn-Ann Algorithm for Low Voltage Application

R. Arul Jose¹, Dr. P. Ebby Darney², Bharathi V³, Udhyami M B⁴

¹ SCAD College of Engineering and Technology, Cheranmahadevi 627414, Tamilnadu, India

^{2,3,4} Department of Electrical and Electronics Engineering

Rajarajeswari college of Engineering, Bangalore, Karnataka, India-560074

aruljoser@gmail.com, pebbydarney@gmail.com, bharathivijay08@gmail.com, mbudhyami@gmail.com

Received: 2022 March 15; **Revised:** 2022 April 20; **Accepted:** 2022 May 10

Abstract

For front end DC/DC conversion in a distributed power system, an LLC resonant converter is proposed in this paper. LLC resonant converters show good efficiency, soft switching and high frequency operation over the traditional conventional converters. The proposed converter has its own advantage of inherently isolated by a high frequency transformer. Also due to high frequency operation, the cost and size of the magnetic components and resonant components are decreased. A robust neural network controller-based LLC resonant converter is used to control the nonlinear phenomenon and to generate low voltage (24V, 192W) for wide range of load by applying variable frequency control. The resonant converter is subjected to Fundamental Harmonic Approximation (FHA), an analysis tool to obtain the DC voltage transfer function. The operation and salient features are discussed and a comparison of the efficiency of this converter with conventional and RBFN controllers shows a prodigious improvement.

Keywords: DC-DC converter, Fundamental Harmonic Approximation (FHA), Series parallel resonant converter (SPRC), Radial basis function network (RBFN), Artificial Neural Network (ANN).

1. Introduction

The role of power converter is to monitor energy with high power transfer efficiency, operating reliability, small size and light weight from a source to an electric load. Via new and creative industries, such as renewable energy, electric cars, lighting and wireless power transfer, the Power Electronics technology continues to extend its applications. Front-end AC-DC converters as shown in figure 1 are required for the majority of off-line applications. Front-end AC-DC converters are extensively used telecommunications, servers, desktop PCs, laptops, gaming systems, and flat panel TVs[1-4]. In the last decade, the portable power electronics system market has been rapidly expanding. When greater power density is required, the converters operate at higher switching frequencies. The size of reactive components can also be decreased. It is difficult for conventional PWM converters to achieve ZVS over the operating range at high efficiency at high frequency [5,6]. Instead of PWM converters, resonant converters are used to overcome much of the disadvantages [8,9,10].

The SPRC shares the benefits of series and parallel resonant converter [7,14]. In high-end applications that requested very high performance, LLC resonant topology was used. Although this topology handles load variations extremely well, the resonant tank needs comprehensive early attempts to design and will have some unique trade-offs [11,12,13]. This Converter eliminates disadvantages, such as the problem of no-load control for series resonant converters and high circulating current for parallel resonant converters at light load.

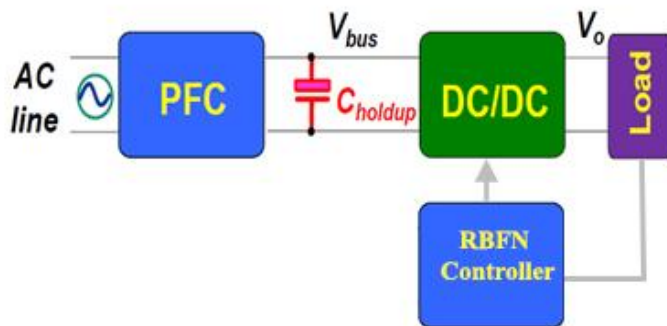


Fig 1 Front end AC-DC converter

The current flowing through the MOSFET and the LC components is independent of the load in this converter. The LLC Resonant converters can additionally implement ZCS to decrease switching loss on the secondary diodes and even ZVS to MOSFET present in primary side converter [15].

DC-DC converters, on the other hand, are thought to be highly dynamic nonlinear systems and changeable operating circumstances [20,21,22]. The Neural Network controller are proficient of addressing uncertainty as well as training and learning from the process itself. Radial Basic Function Network has a faster convergence behaviour than conventional Neural Network, but with a simpler network configuration due to its inherent capability to learn the behavior of systems from a restricted number of samples [23,24].

2. LLC RESONANT DC-DC CONVERTER:

An isolated Resonant Converter is shown in Figure 2. The primary side of resonant converter converts a DC to AC sinusoidal voltage. By means of an appropriate high frequency rectifier, the secondary side converts AC power to DC power. ZVS for MOSFET switches and ZCS for diodes on the secondary side can be realized by the designed LLC resonant converter [16,17,18]. The LLC converter has a MOSFET converter, a resonant tank network, a high frequency transformer, and a network of rectifiers. Alternatively, to control the output voltage, the controller generates a gate signal with variable frequency pulse and constant 50% duty cycle to MOSFETs. The rectifier network rectifies the resonant network's sinusoidal voltage and delivers it to the output point. The power is transferred from source to load by the resonance between two resonant elements, C_r and L_r .

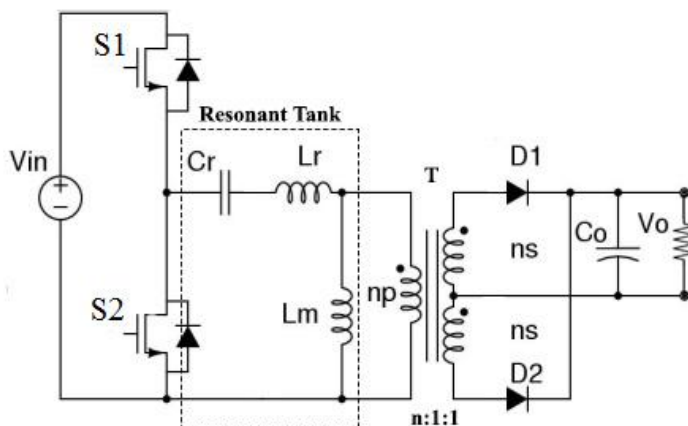


Fig 2 Half bridge LLC resonant DC-DC converter

Thus current flows through the resonant tank network are sinusoidal in form. This enables the DC characteristic of LLC SPRC to be obtained by Fundamental Harmonic Approximation (FHA). Based on FHA, the LLC resonant converter's AC equivalent circuit is derived [10]. It is possible to obtain an AC equivalent load resistance R_{ac} and the fundamental components of resonant tank. As

indicated in Equation 1, the impedance of L_r and L_m resonant inductances and the C_r capacitor varies with variable frequency.

3. FHA ANALYSIS OF LLC CONVERTER

In the ac analysis, square-wave is changed with simple sinusoidal input, and rectifier and filter are replaced with nearly equivalent resistance [12]. Figure 5 demonstrates the corresponding equivalent circuit for the proposed Converter. R_{ac} is the load resistance expressed on the primary side of the transformer.

$$n \cdot V_{out} = \frac{R_{ac} \parallel \omega L_m}{\frac{1}{\omega C_r} + \omega L_r + R_{ac} \parallel \omega L_m} \cdot V_{in} \tag{1}$$

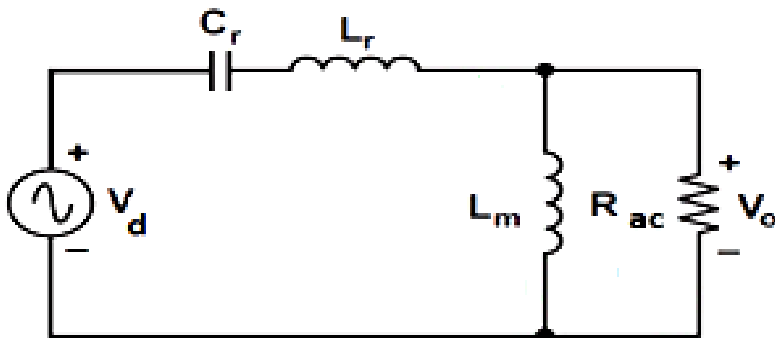


Fig. 5 Equivalent circuit of LLC resonant DC-DC converter

M is the voltage conversion ratio as shown in Equation 2, considering the input waveform as a sinusoidal alternation by the fundamental approximation.

$$M = \frac{2n \cdot V_o}{V_{in}} = \frac{\left(\frac{\omega}{\omega_r}\right)^2 \cdot (m-1)}{\sqrt{\left[\left(\frac{\omega}{\omega_p}\right)^2 - 1\right]^2 + \left(\frac{\omega}{\omega_r}\right)^2 \cdot \left[\left(\frac{\omega}{\omega_r}\right)^2 - 1\right]^2 \cdot ((m-1) \cdot Q)^2}} \tag{2}$$

Where, $m = \frac{L_p}{L_r}$, $\omega_r = \frac{1}{\sqrt{L_r C_r}}$, $\omega_p = \frac{1}{\sqrt{L_p C_r}}$, and $Q = \frac{1}{R_{ac}} \sqrt{\frac{L_r}{C_r}}$ and R_{ac} and V_d can be expressed $\frac{8 \cdot n^2 \cdot V_{out}}{\pi^2 \cdot I_{out}}$ and $\frac{V_{in}}{2}$ respectively.

From Equation 2, ω_p , which is defined by $(L_m + L_r)$ and C_r , and the other by L_r and C_r , is ω_r . By using this equation, as shown in figure 6, the gain curve is designed with respect to the change in switching frequency & load.

$$f_r = \frac{1}{2\pi \sqrt{L_r C_r}} \tag{3}$$

Series parallel resonant frequency

$$f_p = \frac{1}{2\pi\sqrt{(L_r+L_m)C_r}} \quad (4)$$

The switching frequency of the proposed converter should be less than the frequency of series resonant tank and higher than the series parallel resonant tank, so that MOSFETs of primary side can achieve ZVS over the entire operating range. Transformer construction should satisfy the ratio n ,

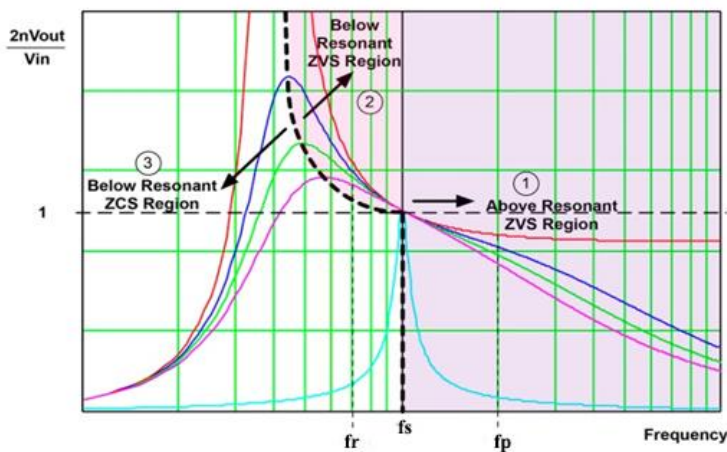


Fig. 6 Gain curve of an LLC converter

$$G_{dc} \leq \frac{V_o}{V_{in(Max-dc)/2}} (@f_{sw} = f_o) \quad (5)$$

$$n \geq \frac{V_{in(Max-dc)}}{2V_o} \quad (6)$$

The determination of k , Q , f_s and n must satisfy the full load requirement of the DC voltage gain. The values of L_r , C_r and L_m can be calculated after the determination of k , Q , f_s and n .

4. IV. RBFN-ANN CONTROLLER

A radial basis functions is used as activation functions in proposed ANN controller [19]. RBF neural networks are the finest when data is noisy [25]. A three-layer RBFN network is implemented with an LLC DC-DC converter shown in Figure 7. There are two input, nine hidden, and one output layers in the proposed network configuration.

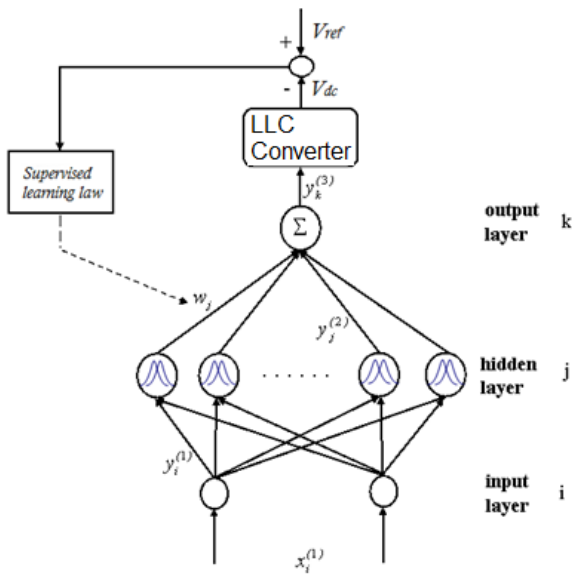


Fig. 7 Neural Network structure

Input Layer: The input layer nodes transfer the inputs to the hidden layer directly.

$$net_i^{(1)} = x_i^{(1)}(N) \tag{12}$$

$$y_i^{(1)}(N) = f_i^{(1)}(net_i^{(1)}(N)) = net_i^{(1)}(N), i = 1, 2 \tag{13}$$

Hidden Layer: The Gaussian function is used here as a membership function, an example of radial basis functions. Then,

$$net_j^{(2)}(N) = -(X - M_j)^T \Sigma_j (X - M_j) \tag{14}$$

$$y_j^{(2)}(N) = f_j^{(2)}(net_j^{(2)}(N)) \tag{15}$$

$$= \exp(-net_j^{(2)}(N)) \quad j = 1 \dots, 9 \tag{16}$$

where $\Sigma_j = \text{diag} [1/\sigma^2_{1j} \ 1/\sigma^2_{2j} \dots 1/\sigma^2_{ij}]^T$ and $M_j = [m_{1j} \ m_{2j} \ \dots \ m_{ij}]^T$ represent the standard deviation and the mean of the Gaussian function.

Output Layer: The single node calculates the number of all incoming inputs.

$$net_k^{(3)} = \sum_j \omega_j y_j^{(2)}(N) \tag{17}$$

$$y_k^{(3)}(N) = f_k^{(3)}(net_k^{(3)}(N)) = net_k^{(3)}(N) \tag{18}$$

where w_j represent the weight between the layers.

To train this network, the gradient descent method is used. By using the training patterns, it modifies the parameters m_{ij} , σ_{ij} and w_j of the network. Adjusting the learning parameters and weight increases machine efficiency [27,28,29]. The goal ANN is to minimise the error E as

$$E = \frac{1}{2} (V_{dc} - V_{ref})^2 \quad (19)$$

5. RESULT AND DISCUSSION

The design is carried out with following specifications. A center-tapped high frequency transformer is used.

- Input DC: 400V
- Output Power: 192W
- Hold-up time: 20ms

Table 1. Design Parameter

Parameters	Design values
Input voltage	400V DC
Output full load	24V/8A
Maximum frequency	100kHz
Minimum frequency	78KHz
L_p	630 μ H
L_r	126 μ H
C_r	20nH

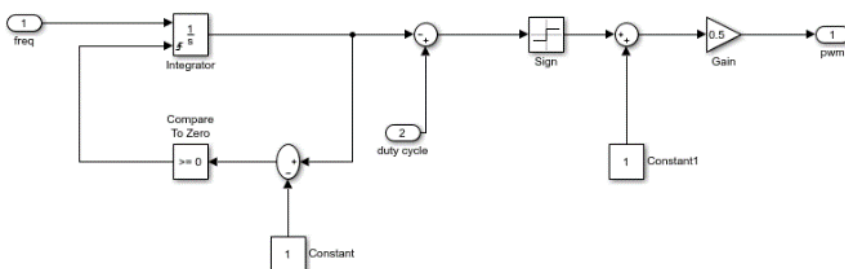


Fig. 8 Variable frequency pulse generation block

Figure 8 shows variable frequency pulse generation block. An integrator block with an external input is used to create a sawtooth signal. The sawtooth signal is then compared to a threshold value given by means of the duty cycle (50%) to create a rectangular signal. Lastly that signal is scaled to a standard output range of 0 to 1 to produce variable frequency pulse. Figure 9 shows the RBFN-ANN block of LLC Converter. The LLC converter's output voltage V_o is compared to the reference voltage V_{ref} , and the comparator output is the error signal that is the artificial neural network controller's input along with the change in error signal. The output of neural network controller block is a variable frequency and this signal is fed to the pulse generation block and the variable pulse output is fed to the converter as a switching signal [26].

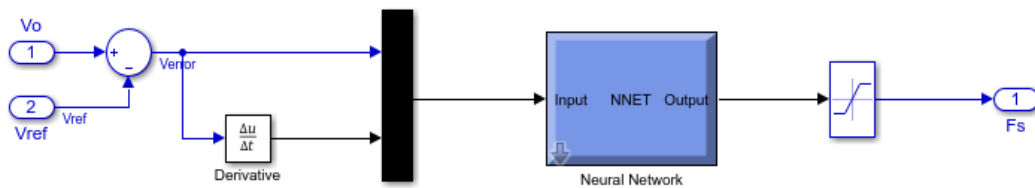


Fig. 9 ANN block for LLC resonant converter

The total weights of 51 are initialized over the interval $[-1, 1]$ with a uniform distribution. The Neural network is trained for 1000 data sets during the learning phase. Figure 10 shows the training efficiency, showing that with training epochs, the RMSE decreases. An RMSE of 0.0119 is derived after 150 training cycles.

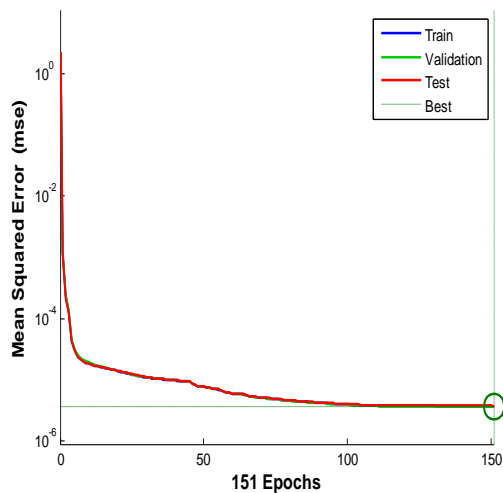


Fig. 10 Training of Neural Network Controller

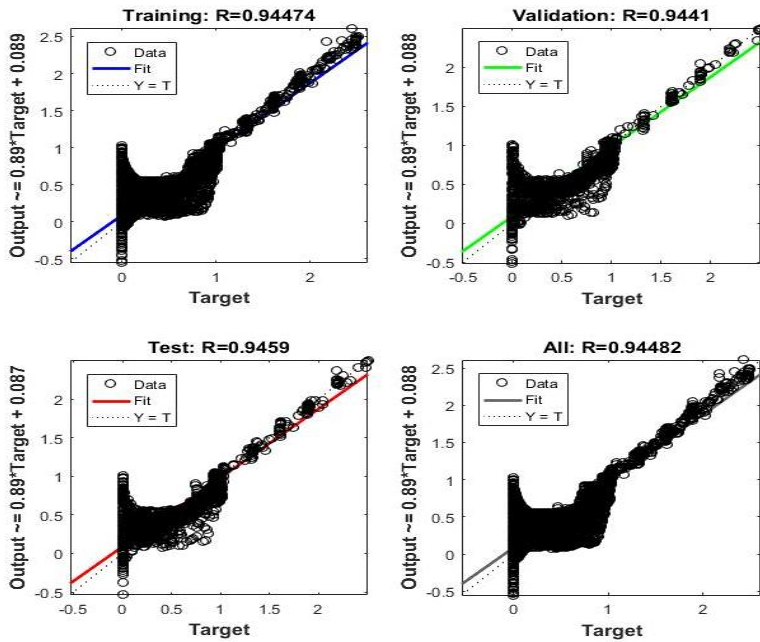


Fig. 11 Training and validation of ANN

LLC Resonant DC-DC converter simulation waveforms proving the ZVS capability of primary switches are shown in Figures 11,12 and 13. Before the MOSFET is on and ZVS is achieved, the MOSFET drain-to-source voltage (VDS) decreases to zero by resonance.

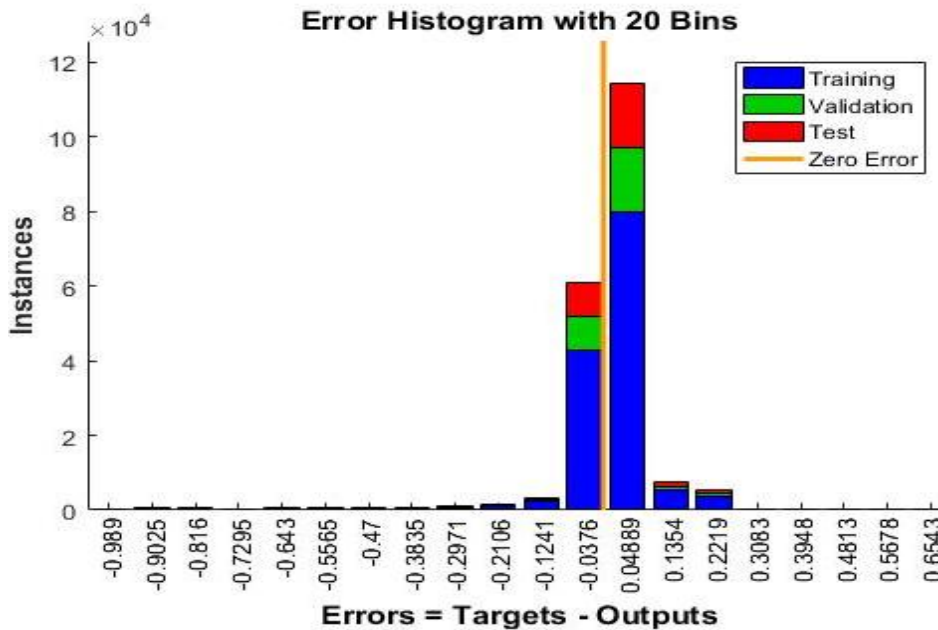


Fig. 12 Error histogram with 20 bins

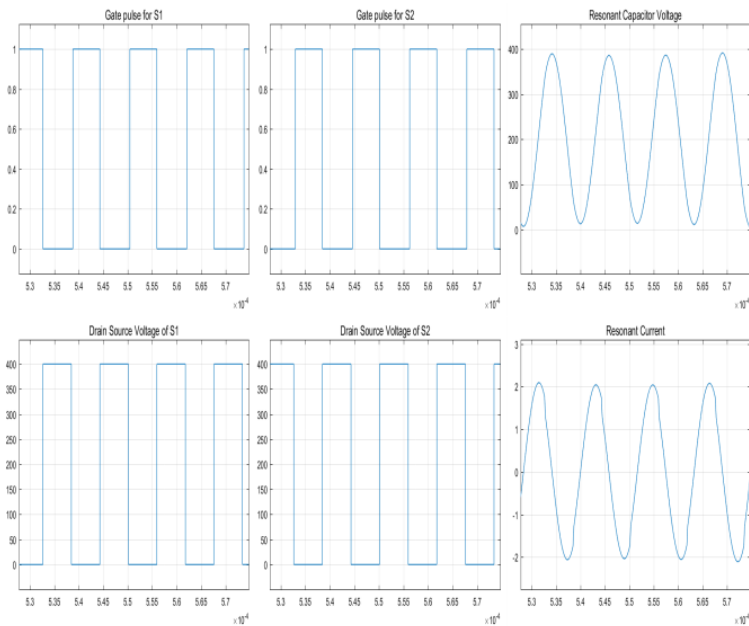


Fig. 13 Gate pulse, drain source voltage, resonant capacitor voltage and resonant current

As observed from simulated results, the switches are not subjected to voltage stress. It is also observed that resonance is established in the circuit without additional inductor that is with the help of leakage inductance. Hence the switching losses are reduced. LLC Resonant DC-DC converter simulation waveforms demonstrating the ZCS ability of secondary diodes are shown in Figure 14. As observed from simulated results, the switches are not subjected to voltage stress. Hence switching loss is reduced in the output rectifier leading to maximum efficiency.

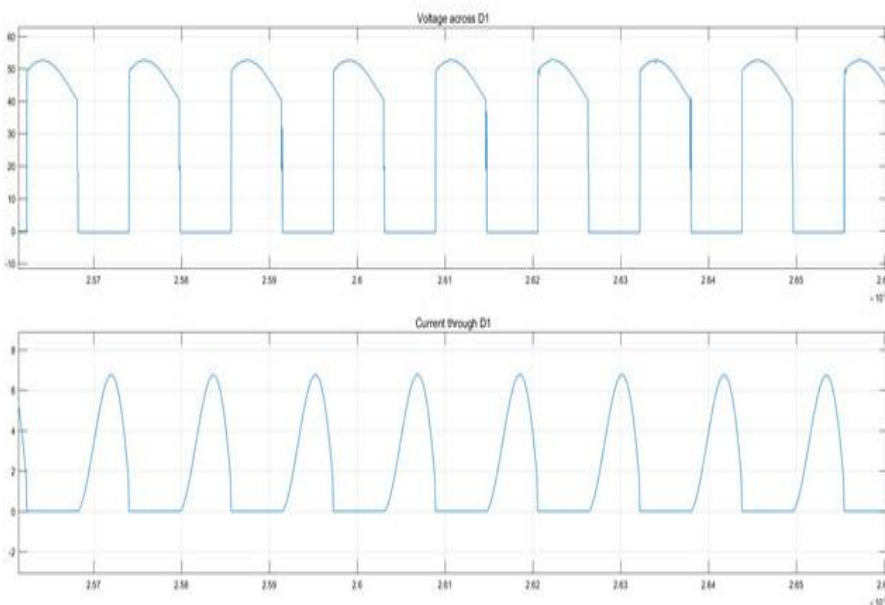


Fig. 14 Voltage and current across secondary rectifier diode

The DC output of 24V/8A is achieved for 100% load and 24V/4A for 50% load, shown in Figure 15. To improve power density, high switching frequencies are used. The variation in switching frequency is narrow, which in turn do not create unwanted harmonics.

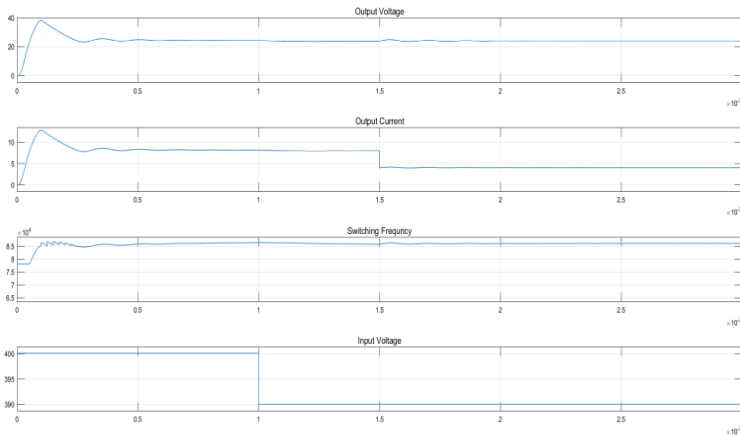


Fig. 15 Load voltage, current and Switching frequency during load and input disturbance

The voltage settling time of raising edge was 0.65ms. Also, output voltage distortions were about 0.02 V with a small overshoot of 12V. These are the improved performance produced by RBFN network compared to conventional PID controller as shown in figure 16.

Table 2. Response of PID and RBFN Controller

	PID controller	RBFN controller
Settling Time(ms)	.95	0.65
Ripple Voltage(V)	0.03	0.02
Peak Overshoot (V)	15	12

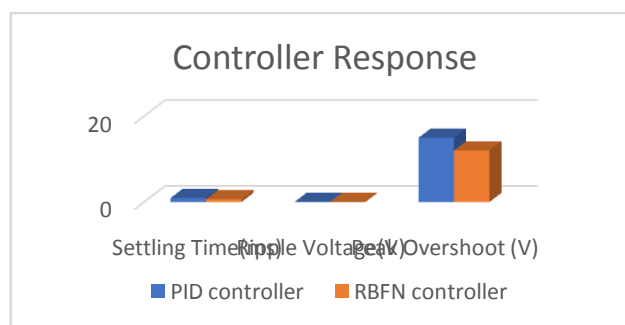


Fig. 16 Response of PID and RBFN Controller

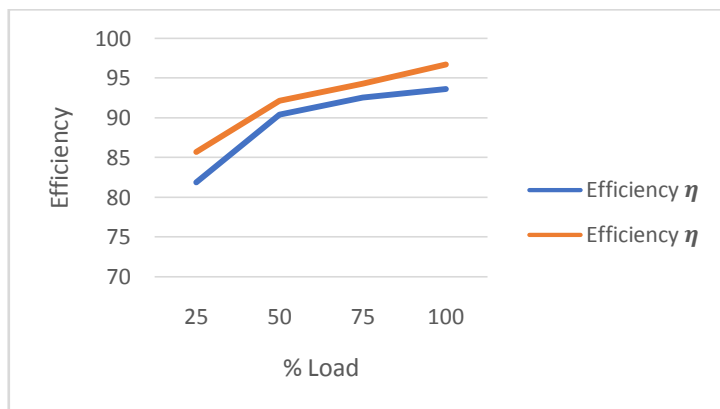


Fig. 17 % Load Vs efficiency

Table 2 shows comparison of PID and ANN Controller response. The performance of the proposed converter under various load condition is shown in Figure 17. The maximum efficiency of proposed LLC resonant converter is found to be 96.73% at rated load condition.

6. CONCLUSION

The proposed LLC Resonant DC-DC converter has improved performance and a wide input range. This converter suits well for an alternative for conventional front-end AC/DC converter. This work proposes a mathematical analysis for the peak gain, which can control the output voltage during the holdup period. Without solving complex differential equations, component stress and soft-switching conditions could be detected by means of FHA analysis. This converter has been proved capable of sustaining ZVS operation. The resonant converter makes use of leakage and stray parts to transmit leakage energy to the output. This allows load independent operating, which is an effective method for low voltage applications.

References

- [1]. Junming Zeng, Guidong Zhang, Samson Shenglong Yu, Bo Zhang, Yun Zhang, “LLC resonant converter topologies and industrial applications — A review” Chinese Journal of Electrical Engineering ,Vol. 6, No.3, 2020, pp.73-84
- [2]. Yuqi Wei, Alan Mantooth, Quanming Luo, Dereje Woldegiorgis, “Control Strategies Generation Mechanism for LLC Resonant Converter” IEEE Energy Conversion Congress and Exposition (ECCE), Oct. 2020

- [3]. Xiaodong Li, A LLC type Dual bridge resonant converter: analysis, design, simulation, and Experimental Results, IEEE Trans. Power Electron, IEEE Trans. Power Electron, Vol.29, No.8, August (2014), pp. 4313-4321
- [4]. Shih-Yu Chen, Zhu Rong Li, Chern-Lin Chen, Analysis and Design of Single-stage AC/DC LLC Resonant Converter, IEEE Trans. Industry Electron, Vol.59, No.3, March (2012), pp 1538-1544
- [5]. Yu Fang, Dehong Xu, Yanjun Zhang, Fengchuan Gao, Lihong Zhu, Design of High Power Density LLC Resonant Converter with Extra Wide Input Range, in Proc. 22nd Annu. IEEE Appl. Power Electron, California, U.S, (2007), pp. 976-981.
- [6]. Sung-Soo Hong, Sang-Ho Cho, Chung-Wook Roh, and Sang-Kyoo Han, Precise Analytical Solution for the Peak Gain of LLC Resonant Converters, Journal of Power Electronics, Vol. 10, No. 6, November (2010), pp. 680-685.
- [7]. Bhat A. K. S, Analysis and design of a series-parallel resonant converter with capacitive output filter, IEEE Transactions on Industry Applications, vol. 27, no. 3 May (1991), pp. 523-530.
- [8]. Kim B. C, Park K. B, Kim C. E, Lee B. H, and Moon G. W, LLC resonant converter with adaptive link-voltage variation for a high power density adapter, IEEE Trans. Ind. Electron., vol. 25, no. 9, September (2010), pp. 2248–2252.
- [9]. ST Microelectronics, Application Note, LLC Resonant Half-Bridge Converter Design Guideline, March (2007).
- [10]. R. Arul Jose, B. Dora Arul Selvi, ‘Performance Investigation of ANFIS controlled LLC resonant converter For DC to DC Energy Conversion’, Journal of Electrical Engineering, vol. 18, no. 2, 2018, pp. 1-8
- [11]. R. Arul Jose, B. Dora Arul Selvi “A LLC Resonant Converter with Neural Network Controller for DC to DC Energy Conversion in Telecom Application”, Journal of Computational and Theoretical Nanoscience, Volume 13, Number 12, December 2016, pp. 9207-9213.
- [12]. R. Arul Jose, B. Dora Arul Selvi “Fuzzy Logic Controller Based LLC Resonant DC-DC Converter” International Journal of Advanced Research Trends in Engineering and Technology, Vol.2, Issue.13, March 2015, pp.1-7.
- [13]. Fairchild Semi conductor, Application Note, Half bridge LLC Resonant Converter Design using FSFR-series Fairchild power switch, September (2007).

- [14]. Fisher R. A, Korman C. S, Franz G. A, Ludwig G. W, Walden J. P, El-Hamamsy S. A, Shenai K, and Kuo M, Performance of low loss synchronous rectifiers in a series-parallel resonant DC-DC converter, Proc. 4th Annu. IEEE Appl. Power Electron. Conf, Baltimore, U.S, (1989), pp. 240-246.
- [15]. Yang B, Lee F. C, Zhang A. J, and Huang G, LLC resonant converter for front end DC/DC conversion," Proc. 17th Annu. IEEE Appl. Power Electron. Conf, Texas, U.S, (2002), pp. 1108-1112.
- [16]. Fu D, Lu B, and Lee F. C, 1 MHz high efficiency LLC resonant converters with synchronous rectifier, Proc. IEEE Power Electron. Spec. Conf, Florida, U.S, (2007), pp. 2404-2410.
- [17]. Abdel-Rahim, O.; Alamir, N.; Orabi, M. Mohamed Ismeil Fixed-frequency phase-shift modulated PV-MPPT for LLC resonant converters. *J. Power Electron.* 2019, 20, 279–291.
- [18]. Alamir, N.; Abdel-Rahim, O.; Ismeil, M.; Orabi, M.; Kennel, R. Fixed Frequency Predictive MPPT for Phase-Shift Modulated LLC Resonant Micro-Inverter. In Proceedings of the 2018 20th European Conference on Power Electronics and Applications (EPE'18 ECCE Europe), Riga, Latvia, 17–21 September 2018; pp. 1–9.
- [19]. Whei-Min Lin, Chih-Ming Hong, Chiung-Hsing Chen, Neural-Network-Based MPPT Control of a Standalone hybrid power generation system, *IEEE Trans. Power Electron*, vol 26, no. 12, Dec (2011), pp. 3571-3581
- [20]. H. Maruta, M. Motomura, K. Ueno, F. Kurokawa, "Reference modification control DC-DC converter with neural network predictor", Proc. of IEEE COMPEL, pp. 1-4, June 2012.
- [21]. H. Maruta, M. Motomura, F. Kurokawa, "A Novel Timing Control Method for Neural Network Based Digitally Controlled DC-DC Converter", Proc. EPE(ECCE Europe), pp. 1-8, 2013
- [22]. T. Fukuda, T. Shibata, "Theory and applications of neural networks for industrial control systems", *IEEE Trans. Ind. Electron.*, vol. 39, pp. 472-491, 1992.
- [23]. Weiming Li, Xiao-Hua Yu, "Improving DC power supply efficiency with neural network controller", in: Proceedings of the IEEE International Conference on Control and Automation, May 2007, pp. 1575–1580.
- [24]. J. M. Quero, J. M. Carrasco, L. G. Franquelo, "Implementation of a neural controller for the series resonant converter", *IEEE Trans. Ind. Electron.*, vol. 49, no. 3, pp. 628-639, Jun. 2002.
- [25]. J. M. Quero, E. F. Camacho, "Neural generalized predictive self-tuning controllers", Proc. IEEE Int. Conf. Systems Engineering, pp. 160-163, 1990.

- [26]. J. M. Quero, E. F. Camacho, L. G. Franquelo, "Neural networks for constrained predictive control", *IEEE Trans. Circuits Syst.*, vol. 40, pp. 621-626, Sept. 1993.
- [27]. J. M. Carrasco, J. M. Quero, F. P. Ridaó, M. A. Perales, L. G. Franquelo, "Sliding mode control of a DC/DC PWM converter with PFC implemented by neural networks", *IEEE Trans. Circuits Syst.*, vol. 44, pp. 743-749, Aug. 1997
- [28]. J. M. Quero, J. M. Carrasco, L. G. Franquelo, "A neural controller for quasi resonant converters", *Proc. 4th European Conf. Power Electronics and Applications*, vol. 4, pp. 207-211, 1991.
- [29]. J. M. Quero, J. M. Carrasco, L. G. Franquelo, "Adaptive energy feedback control for resonant converter using neural networks", *Proc. IEEE PESC'92*, vol. 2, pp. 800-806, 1992.